STEM CELLS®

STEM CELL TECHNOLOGY: EPIGENETICS, GENOMICS, PROTEOMICS AND METABONOMICS

Long Noncoding RNA H19 Promotes Osteoblast Differentiation Via TGF-β1/Smad3/HDAC Signaling Pathway by Deriving miR-675

YIPING HUANG,[a] YUNFEI ZHENG,[b] LINGFEI JIA,[b,c] WEIRAN LI[a]

Key Words. Mesenchymal stem cells • Osteoblast differentiation • lncRNA • miRNA • H19 • miR-675

[a]Department of Orthodontics, [b]Department of Oral and Maxillofacial Surgery, and [c]Central Laboratory, Peking University School and Hospital of Stomatology, Beijing, People's Republic of China

Correspondence: Lingfei Jia, M.D., Ph.D., Central Laboratory, Peking University School and Hospital of Stomatology, 22 Zhongguancun Avenue South, Haidian District, Beijing 100081, People's Republic of China. Telephone: +86-10-82195778; Fax: +86-10-82193402; e-mail: jialingfei1984@sina.com; and Weiran Li, D.D.S., Ph.D., Department of Orthodontics, Peking University School and Hospital of Stomatology, 22 Zhongguancun Avenue South, Haidian District, Beijing 100081, People's Republic of China. Telephone: +86-10-82195332; Fax +86-10-82195336; e-mail: weiranli2003@163.com

Received April 6, 2015; accepted for publication August 24, 2015; first published online in STEM CELLS *EXPRESS* September 29, 2015.

1066-5099/2015/$30.00/0

http://dx.doi.org/10.1002/stem.2225

ABSTRACT

Long noncoding RNAs (lncRNAs) are emerging as important regulatory molecules at the transcriptional and post-transcriptional levels and may play essential roles in the differentiation of human bone marrow mesenchymal stem cell (hMSC). However, their roles and functions remain unclear. Here, we showed that lncRNA H19 was significantly upregulated after the induction of osteoblast differentiation. Overexpression of H19 promoted osteogenic differentiation of hMSCs in vitro and enhanced heterotopic bone formation in vivo, whereas knockdown of H19 inhibited these effects. Subsequently, we found that miR-675, encoded by exon1 of H19, promoted osteoblast differentiation of hMSCs and was partially responsible for the pro-osteogenic effect of H19. Investigating the underlying mechanism, we demonstrated that H19/miR-675 inhibited mRNA and protein expression of transforming growth factor-β1 (TGF-β1). The downregulation of TGF-β1 subsequently inhibited phosphorylation of Smad3. Meanwhile, H19/miR-675 downregulated the mRNA and protein levels of histone deacetylase (HDAC) 4/5, and thus increased osteoblast marker gene expression. Taken together, our results demonstrated that the novel pathway H19/miR-675/TGF-β1/Smad3/HDAC regulates osteogenic differentiation of hMSCs and may serve as a potential target for enhancing bone formation in vivo. STEM CELLS *2015;33:3481–3492*

SIGNIFICANCE STATEMENT

Long noncoding RNAs (lncRNAs) are emerging as important regulatory molecules in biology control and pathology. However, their roles and functions in osteogenic differentiation of mesenchymal stem cell (MSC) remain unclear. Our studies provide important insights into the pro-differentiation effect of lncRNA H19 in osteogenesis both in vitro and in vivo. miR-675 is partially responsible for this pro-osteogenic effect of H19 via the transforming growth factor-β1 (TGF-β1)/Smad3/histone deacetylase (HDAC) pathway. These findings provide important clues for understanding the role of lncRNA-miRNA-mRNA functional network in osteogenic differentiation, and would be helpful in developing stem cell-based therapy for bone defect.

INTRODUCTION

MSCs have the capacity of self-renewal and multilineage differentiation, and they are therefore useful to regenerate or repair bone tissue [1, 2]. Human bone marrow MSCs (hMSCs) have the advantages of availability, culture expansion, and low immunogenic properties [3], and thus they are commonly used in clinical applications [4]. Despite a great deal of research on controlling hMSC differentiation into specific lineages by modulating cell signaling pathways, the precise molecular mechanisms of differentiation remain unclear.

Non-protein-coding RNAs (ncRNAs) encoded in the human genome serve as important regulatory transcripts in biological control and pathology [5]. A class of small ncRNAs, including miR-29b [6], miR-34a [7], miR-140 [8], and miR-542 [9], have been identified as positive or negative regulators in hMSC osteogenic differentiation. By contrast, the roles and functions of long noncoding RNAs (lncRNAs), tentatively defined as ncRNAs >200 nt in length [10, 11], are still largely unknown in hMSC osteogenic differentiation. Recently, the differential lncRNA expression profiles of undifferentiated and differentiated cells during osteogenesis were established using an lncRNA microarray, and 1,206 differentially expressed lncRNAs were

identified. H19 is among the strongly upregulated groups, and it is considered to play an important role in the osteogenic differentiation process [12]. It has been shown that H19 is a paternally imprinted gene that does not encode a protein, but rather a 2.3-kb H19 ncRNA [13]. Moreover, H19 is highly conserved in evolution with a very low mutation rate in exons, indicative of an important biological function [14]. However, the function and underlying mechanisms by which H19 contributes to osteogenic differentiation require further investigation.

One way that lncRNAs acquire functionality is by acting as precursors of small RNAs capable of regulatory functions, such as miRNAs [15–17]. Indeed, H19 is a primary miRNA precursor for microRNA-675 (miR-675) and generates two mature miRNAs, namely miR-675-5p and miR-675-3p, in a classic Drosha and Dicer splicing-dependent manner. It has been suggested that these miRNAs confer functionality on H19 [18–20]. Therefore, we explored the roles and functions of H19/miR-675 in the osteogenic differentiation of hMSCs and investigated the underlying mechanism.

In this study, we found that the expression of H19 and miR-675 were significantly increased during osteogenic differentiation of hMSCs. We demonstrated that H19 promoted osteogenesis, and its pro-osteogenic function was at least partially mediated by miR-675. Moreover, our results showed that miR-675 not only downregulated TGF-β1 and subsequently inhibited Smad3 phosphorylation, but also downregulated HDAC 4/5 to reduce the recruitment of HDAC(s) to the Runt-related transcription factor 2 (Runx2)-binding DNA sequence. These results increase our understanding on the role of the lncRNA-miRNA-mRNA functional network in osteogenesis and bone development.

Materials and Methods

Cell Culture

Primary hMSCs (ScienCell, San Diego, CA, http://sciencellonline.com) were cultured at subconfluent densities in growth medium (GM) consisting of α-minimum essential medium supplemented with 10% fetal bovine serum and 1% antibiotics. Osteoblast (OB) differentiation of hMSCs was induced after 70%–80% confluence using standard GM supplemented with 100 nM dexamethasone, 200 μM L-ascorbic acid, and 10 mM β-glycerophosphate. The osteogenic medium (OM) was changed every 2 days, and cells were harvested at the indicated times after OB differentiation. The 293T cells were obtained from American Type Culture Collection (Manassas, VA, http://www.atcc.org) and cultured in Dulbecco's modified Eagle's medium supplemented with 10% fetal bovine serum and 1% antibiotics.

Lentivirus Infection and Establishment of Stably Expressing Transfectants

The full-length lncRNA H19 (Gene Bank accession number, NR_002196.1) cDNA cloned into the lentivector-transferred plasmid pLVX-IRES-ZsGreen (Clontech Laboratories, Inc., Tokyo, Japan, http://www.clontech.com) was obtained from Integrated Biotech Solutions Company (Ibsbio, Co., Ltd., Shanghai, People's Republic of China, http://www.ibsbio.com) and named Lenti-H19. Site-directed mutagenesis of the H19 sequences was performed using the Site-Directed Mutagenesis Kit (SBS Genetech, Beijing, People's Republic of China, http://www.sbsbio.com) and named Lenti-H19-mut, which carried mutations in the sequences of miR-675-5p and miR-675-3p, as follows: TGG TGC GGA GAG GGC CCA CAG TG was changed to TCC ACG CGA GAG GGC CCA CAG TG, and CUG UAU GCC CUC ACC GCU CA was changed to GAC ATA GCC CUC ACC GCU CA. The recombinant vector or the control vector was triple-transfected with the packaging vectors psPAX2 and pMD2.G into the 293T cells to produce the lentiviruses. Two days later, the supernatants were collected, filtered, and concentrated as described previously [21, 22].

Recombinant lentiviruses targeting H19 (Lenti-shH19-1 and Lenti-shH19-2) and the scramble control (Lenti-shNC) were obtained from GenePharma, Co. (Shanghai, People's Republic of China, http://www.genepharma.com/En/). Recombinant lentiviruses containing pre-miR-675 (Lenti-miR-675) and the control (Lenti-miR-NC), miR-675 inhibitor (Lenti-anti-miR-675), and the control (Lenti-anti-NC) were obtained from Integrated Biotech Solutions, Co. (Ibsbio, Co.). All lentivirus vectors contained the gene for green fluorescent protein (GFP).

The viruses were used to infect hMSCs and establish stably expressing transfectants, as described previously [22]. Transfection of the hMSCs was performed by exposing them to dilutions of the viral supernatant in the presence of polybrene (5 μg/ml) for 24 hours. The infected cells were screened and sorted by fluorescence-activated cell sorting (FACS) based on the expression of ZsGreen or GFP. The sorted cells were then used as the stably expressing model in subsequent experiments.

Alkaline Phosphatase Staining and Activity

Alkaline phosphatase (ALP) staining and activity were performed as described previously [23, 24]. ALP staining was performed according to the protocol of the NBT/BCIP staining kit (CoWin Biotech, Beijing, People's Republic of China, http://www.cwbiotech.com). Briefly, the cultured cells were rinsed with PBS and fixed in 4% paraformaldehyde for 30 minutes. The cell layer was then washed three times with phosphate buffered saline (PBS) and incubated in alkaline solution for 20 minutes at 37°C.

ALP activity was analyzed using an ALP activity colorimetric assay kit (Biovision, Milpitas, CA, http://www.biovision.com). The cultured cells were rinsed three times with PBS, followed by 1% Triton X-100, and then scraped into distilled water. This was followed by three cycles of freezing and thawing. ALP activity was determined at 405 nm using *p*-nitrophenyl phosphate as substrate. Total protein content was determined in the same sample with the bicinchoninic acid (BCA) method using the Pierce protein assay kit (Thermo Fisher Scientific, Rockford, IL, http://www.thermofisher.com). ALP activity relative to the control treatment was calculated after normalization to the total protein content.

Alizarin Red S Staining and Quantification

Mineralization was determined by Alizarin red S staining, as described previously [23, 24]. The cultured cells were fixed in 95% ethanol for 30 minutes and then stained with 0.1% Alizarin red S pH 4.2 (Sigma-Aldrich, Saint Louis, MO, http://www.sigmaaldrich.com) for 20 minutes at room temperature. For quantitative assessment of the degree of mineralization, the stain was eluted by 100 mM cetylpyridinium chloride (Sigma-

Aldrich) for 1 hour and quantified by spectrophotometric absorbance at 570 nm. Alizarin red S intensity relative to the control treatment was calculated after normalization to the total protein content.

von Kossa Staining

Cells cultured for 14 days under differentiation conditions were assayed for mineralization using the histochemical von Kossa staining method [25]. Briefly, cells were washed in PBS and fixed with 4% paraformaldehyde for 30 minutes. Cells were then incubated with 5% silver nitrate solution for 30 minutes in the dark, followed by exposure to UV light. Unincorporated silver nitrate was removed using 5% sodium thiosulfate, followed by several washes with water.

Immunofluorescence Staining

Immunofluorescence staining was performed as described previously [26]. Cells grown on sterile glass coverslips were fixed with 4% paraformaldehyde for 30 minutes, permeabilized with 0.1% Triton X-100 for 15 minutes, and then blocked with 3% bovine serum albumin (BSA; Sigma-Aldrich) for 30 minutes. Thereafter, cells were incubated with primary antibody at 4°C overnight and incubated in the specified secondary antibodies for 1 hour. Nuclei were counterstained with DAPI, and the coverslips were mounted on a glass slide. Images were captured with a LSM 5 EXCITER confocal imaging system (Carl Zeiss, Jena, Germany, http://www.zeiss.com).

RNA Oligoribonucleotide and Chemicals

A chemically modified double-stranded miR-675-5p mimic, miR-675-3p mimic, and the corresponding miRNA mimic control were obtained from RiboBio, Co. (Guangzhou, People's Republic of China, http://www.ribobio.com). The sequences are listed in Supporting Information Table S1. The recombinant human TGF-β1 was purchased from R&D Systems (Minneapolis, MN, http://www.biotechniques.com) and dissolved in citric acid (pH 4.3). Trichostatin A (TSA) from Sigma-Aldrich was dissolved in dimethyl sulfoxide.

Transient Transfection

Cells at 70%–80% confluence were transfected with miR-675-3p mimic, miR-675-5p mimic, or miRNA mimic control at 100 nM using Lipofectamine 2000 (Invitrogen, Carlsbad, CA, http://www.thermofisher.com/cn/en/home/brands/invitrogen.html) according to the manufacturer's procedure. The cells were harvested 24 hours after transfection for mRNA analysis.

Reporter Vectors

Predicted miR-675 target genes and their target binding sites were investigated using RNA22 software [27]. The reporter vectors were constructed by Integrated Biotech Solutions, Co. Briefly, the 5′UTR of the TGF-β1 mRNA containing the predicted miR-675-5p binding sites was synthesized ($\sim$200 bp) and cloned into a psiCHECK-2 vector (Promega, Madison, WI, http://www.promega.com) in the 5′-upstream of Renilla luciferase similar as reported previously [28]. The miR-675-3p target sequences in the coding region (CD) of TGF-β1 mRNA were synthesized ($\sim$200 bp) and cloned into a position downstream of a Renilla luciferase open reading frame, as described previously [22]. Site-directed mutagenesis of selected putative seeding sequence regions was performed using a Site-Directed Mutagenesis Kit (SBS Genetech). All constructs were confirmed by DNA sequencing.

Dual Luciferase Reporter Assay

Luciferase assays were performed as described previously [28]. Briefly, the 293T cells grown in a 48-well plate were transfected with 40 ng of TGF-β1 luciferase reporter and 100 nM miR-675-5p/miR-675-3p mimic or control using Lipofectamine 2000. The Renilla and Firefly luciferase activities were measured 24 hours after transfection using the Dual Luciferase Reporter Assay System (Promega). The light intensity from Renilla luciferase was normalized by Firefly luciferase.

RNA Isolation and Quantitative Reverse-Transcription (qRT-PCR)

Total RNA was extracted using TRIzol reagent (Invitrogen) according to the manufacturer's procedure, and then reverse-transcribed into cDNA using a cDNA Reverse Transcription Kit (Applied Biosystems, Foster City, CA, http://www.thermofisher.com/cn/en/home/brands/applied-biosystems.html). Quantitative PCR was conducted with the ABI Prism 7500 real-time PCR System (Applied Biosystems). The following thermal settings were used: 95°C for 10 minutes followed by 40 cycles of 95°C for 15 seconds and 60°C for 1 minute. The primers used for H19, miR-675, TGF-β1, ALP, osteocalcin (OCN), Runx2, HDAC4/5, U6 (internal control for miRNAs), and glyceraldehyde 3-phosphate dehydrogenase (GAPDH, internal control for mRNAs and lncRNAs) are listed in Supporting Information Table S1. The data were analyzed using the $2^{-\Delta\Delta Ct}$ relative expression method as described previously [27].

Western Blot Analysis

Western blot analysis was performed as described previously [27]. Primary antibodies against TGF-β1 (Cell Signaling Technology, Beverly, MA, http://www.cellsignal.com), p-Smad3 (Santa Cruz Biotechnology, Santa Cruz, CA, http://www.scbt.com), Smad3 (Santa Cruz Biotechnology), HDAC4 (Cell Signaling Technology), HDAC5 (Cell Signaling Technology), Runx2 (Cell Signaling Technology), GAPDH (Santa Cruz Biotechnology), and β-actin (Santa Cruz Biotechnology) were diluted 1:1,000. The intensities of the bands obtained by Western blot analysis were quantified using ImageJ software (http://rsb.info.nih.gov/ij/). The background was subtracted, and the signal of each target band was normalized to that of the GAPDH or β-actin band.

In Vivo Heterotopic Bone Formation Assay

The hMSCs were induced under OM for 1 week before the in vivo study. The cells were resuspended and incubated with 7 mm $\times$ 5 mm $\times$ 2 mm Bio-Oss Collagen (Geistlich, GEWO GmbH, Baden-Baden, Germany, http://www.geistlich-na.com/en-us/) scaffolds for 1 hour at 37°C followed by centrifugation at 150*g* for 5 minutes, and then implanted subcutaneously on the back of 5-week-old BALB/c homozygous nude (nu/nu) mice (five mice per group), as described previously [23, 24, 29, 30]. Implants were harvested after 8 weeks and fixed in 4% paraformaldehyde. All animal experiments were approved by the Peking University Animal Care and Use Committee.

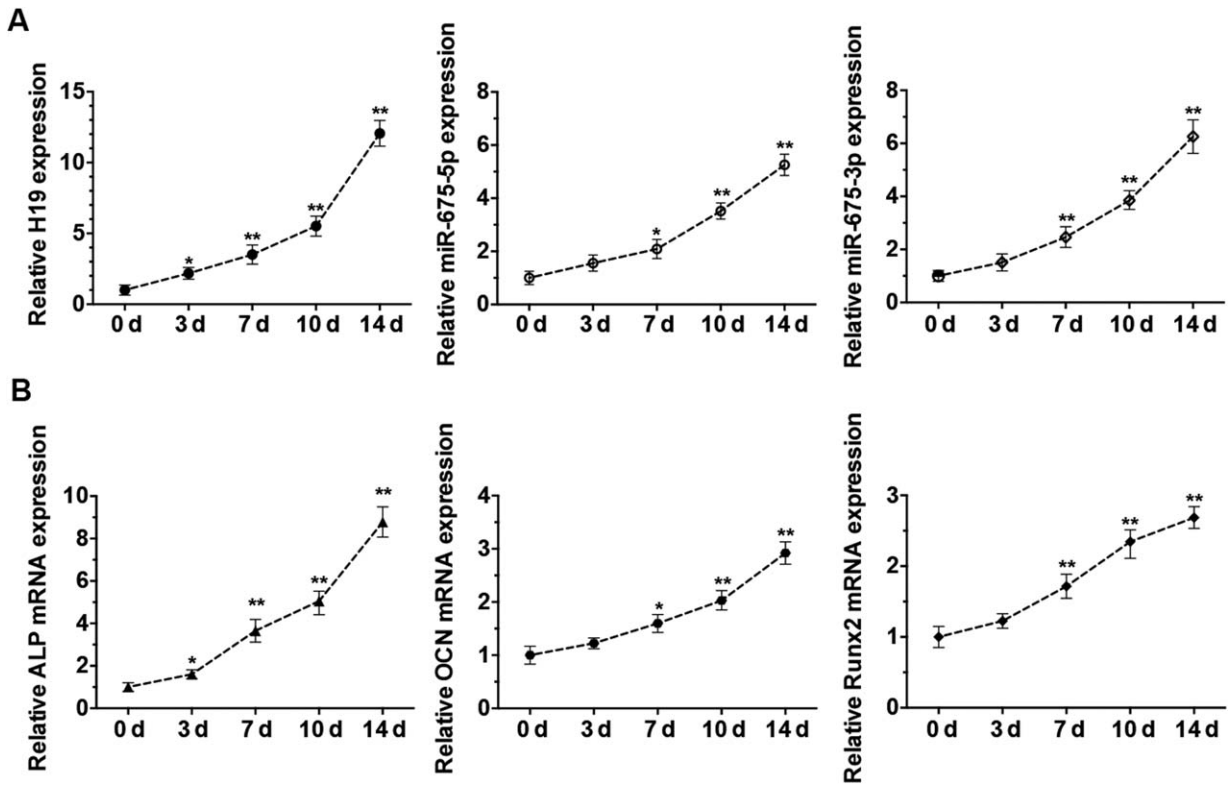

Figure 1. Expression patterns of lncRNA H19 and its encoded miR-675 during osteoblast differentiation of human mesenchymal stem cells (hMSCs). **(A):** Left: relative expression of H19 as determined by qRT-PCR analysis during osteoblast differentiation of hMSCs at days 0, 3, 7, 10, and 14. RNA expression at indicated time points was normalized to day 0. GAPDH was used as an internal control. Middle and Right: relative miR-675-5p and miR-675-3p transcript levels at the indicated time points. U6 was used as an internal control. **(B):** Relative mRNA expression normalized by GAPDH for osteoblastic markers of ALP, Runx2, and OCN on selected days, as in (A). Results are presented as the mean ± SD (*, $p < .05$; **, $p < .01$ compared with control hMSCs at the indicated days). Abbreviations: ALP, alkaline phosphatase; OCN, osteocalcin; Runx2, Runt-related transcription factor 2.

Micro-CT analysis

Micro-CT analysis of specimens was performed using a high-resolution Inveon Micro-CT (Siemens, Munich, Germany, http://www.siemens.com). Briefly, the x-ray source was set at 80 kV, with a node current of 500 μA and an exposure time of 500 ms for each of the 360 rotational steps. Image slices were then reconstructed using micro-CT image analysis software (Inveon Research Workplace). The three-dimensional reconstruction and volume quantification of the ectopic bone were performed using standardized thresholds as described previously [29–32]. The region of interest was selected, and the lower and upper threshold values for bone were set. Relevant parameters, including bone mineral density (BMD, mg/ml) and the ratio of new bone volume to existing tissue volume (BV/TV), were calculated.

H&E Staining and Immunohistochemical Analysis

The specimens were decalcified in 10% ethylene diamine tetraacetic acid (pH 7.4) for 1 month, followed by dehydration and embedding in paraffin. Sections (5 μm) were cut and stained with hematoxylin and eosin (H&E). Meanwhile, sections were evaluated by immunohistochemical analysis, as described previously [26]. The specimens were blocked with 3% BSA for 30 minutes and then incubated with primary antibody against OCN (Santa Cruz Biotechnology) at 4°C overnight. Then, sections were processed using the ABC detection kit (Vector Laboratories, Burlingame, CA, http://www.vectorlabs.com) and visualized under an Olympus BX51 light microscope equipped with an Olympus DP70 camera (Olympus, Co., Tokyo, Japan, http://www.olympus-global.com/en/).

Statistical Analysis

Statistical analyses were performed using SPSS version 16.0 (SPSS, Chicago, IL, http://www.spss.com). All data are expressed as the mean ± SD from at least three independent experiments. Differences between groups were analyzed using Student's *t* test. In cases of multiple-group testing, one-way analysis of variance was conducted. A two-tailed value of $p < .05$ was considered statistically significant.

Results

lncRNA H19 and Its Encoded miR-675 Are Upregulated During OB Differentiation of hMSCs

To investigate the functionality of H19 and H19-derived miR-675, we detected their dynamic expression profiles in hMSCs after induction to the osteogenic lineage. H19 expression was gradually upregulated during OB differentiation, reaching >10-fold on day 14 (Fig. 1A). The expression pattern of miR-675 showed a trend similar to H19 with more than fourfold upregulation on day 14 in hMSCs during OB differentiation in vitro (Fig. 1A). Quantitative RT-PCR results showed that the

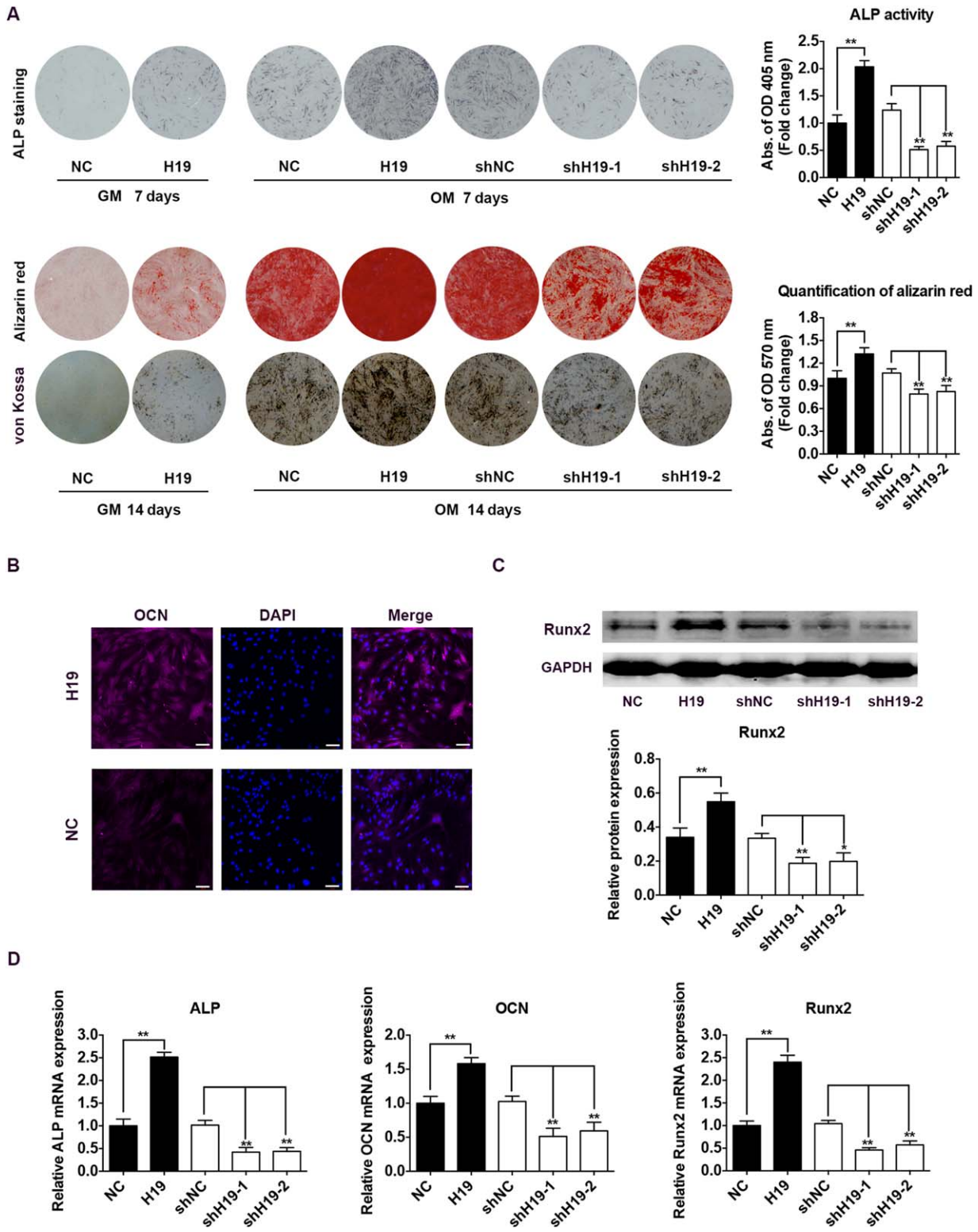

Figure 2. H19 promoted osteogenic differentiation of human mesenchymal stem cells. **(A):** Upper: images of ALP staining in the NC, H19, shNC, shH19-1, and shH19-2 groups. Cells were cultured in GM or OM for 7 days. Lower: images of Alizarin red staining and von Kossa staining for mineralized matrix in the NC, H19, shNC, shH19-1, and shH19-2 groups. Cells were cultured in GM or OM for 14 days. Histograms show ALP activity and quantification of Alizarin red staining by spectrophotometry (normalized to the NC groups). **(B):** Confocal microscopy of OCN with DAPI counterstaining in NC and H19 groups after induction to the osteogenic lineage at day 7. Scale bars = 50 μm. **(C):** Western blot analysis of protein expression of Runx2 and the internal control GAPDH at day 7 of osteoblast (OB) induction. Histograms show the quantification of band intensities. **(D):** Relative mRNA expression of ALP, OCN, and Runx2 measured by qRT-PCR at day 7 of OB induction. GAPDH was used for normalization. Results are presented as the mean ± SD (*, $p < .05$; **, $p < .01$). Abbreviations: ALP, alkaline phosphatase; GAPDH, glyceraldehyde 3-phosphate dehydrogenase; GM, growth medium; NC, negative control; OCN, osteocalcin; OM, osteogenic medium; Runx2, Runt-related transcription factor 2.

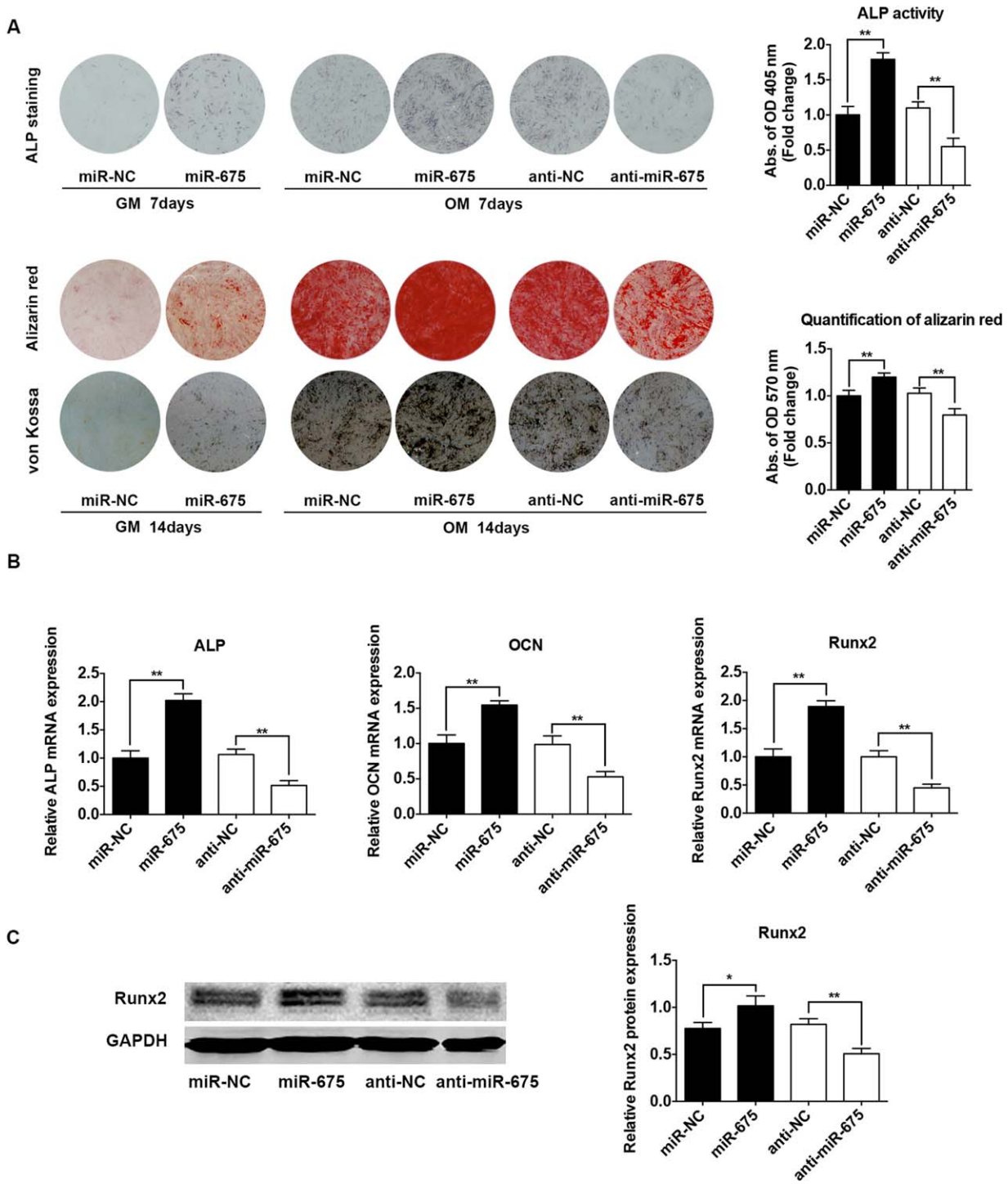

Figure 3. miR-675 promoted osteoblast differentiation of human mesenchymal stem cells. **(A):** Upper: images of ALP staining in the miR-NC, miR-675, anti-NC, and anti-miR-675 groups. Cells were cultured under GM or OM for 7 days. Lower: images of Alizarin red staining and von Kossa staining in the miR-NC, miR-675, anti-NC, and anti-miR-675 groups. Cells were cultured under GM or OM for 14 days. Histograms show ALP activity and quantification of Alizarin red staining by spectrophotometry (normalized to the miR-NC groups). **(B):** Relative mRNA expression of ALP, OCN, and Runx2 at day 7 of osteoblast (OB) induction (by qRT-PCR; normalized by GAPDH). **(C):** Western blot analysis (left) and quantification (right) of protein expression of Runx2 and GAPDH at day 7 of OB induction. Data are presented as the mean ± SD (*, $p < .05$; **, $p < .01$). Abbreviations: ALP, alkaline phosphatase; GAPDH, glyceraldehyde 3-phosphate dehydrogenase; GM, growth medium; NC, negative control; OCN, osteocalcin; OM, osteogenic medium; Runx2, Runt-related transcription factor 2.

mRNA expression of early stage osteogenic markers Runx2 and ALP and the mineralization stage marker OCN was significantly upregulated during osteogenesis (Fig. 1B).

lncRNA H19 Promotes OB Differentiation of hMSCs

Lentivirus was used to overexpress H19 (Lenti-H19) or knockdown H19 (Lenti-shH19-1 and Lenti-shH19-2) in hMSCs, and

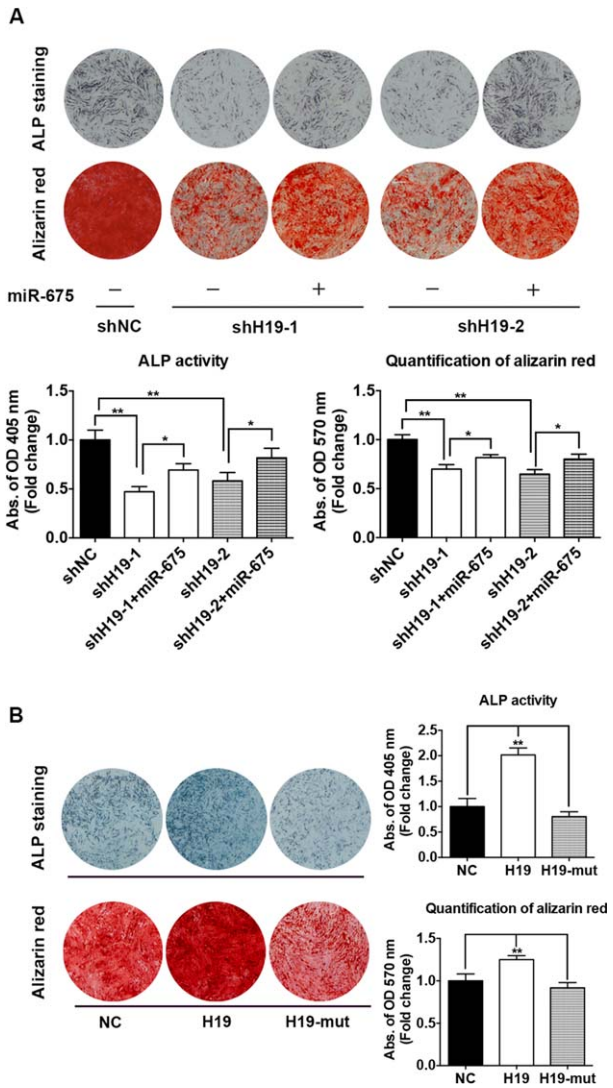

Figure 4. miR-675 was partially responsible for the pro-osteogenic effect of H19. **(A):** Lenti-miR-675 was used to overexpress miR-675 in human mesenchymal stem cells (hMSCs) stably expressing shH19. Upper: images of ALP staining on day 7 of osteoblast (OB) induction and Alizarin red staining on day 14 of OB induction. Lower: ALP activity (left) and quantification of Alizarin red staining (right) in each indicated group normalized to the shNC group. **(B):** Lenti-H19-Mut carried mutations in sequences of miR-675 and was transfected into hMSCs. Upper: images of ALP staining (left) and ALP activity (right) after induction to the osteogenic lineage at day 7. Lower: images (left) and quantification (right) of Alizarin red staining after induction to the osteogenic lineage at day 14. The ALP activity and quantification of Alizarin red staining were normalized to the NC group. Data are presented as the mean ± SD (*, $p < .05$; **, $p < .01$). Abbreviations: ALP, alkaline phosphatase; NC, negative control.

stably expressing cells were sorted into NC, H19, shNC, shH19-1, and shH19-2 groups. The efficiency of lentiviral transduction was >90% (Supporting Information Fig. S1A). Real-time PCR analysis confirmed more than eightfold expression in the H19-overexpression group and a ~70% decrease in the H19-knockdown groups compared to the control group (Supporting Information Fig. S1B).

After OB induction for 7 days, the expression and activity of ALP were increased by H19 overexpression and decreased by H19 knockdown (Fig. 2A). Following OB induction for 14 days, matrix mineralization as revealed by Alizarin red and von Kossa staining was enhanced in H19-upregulated cells and reduced in H19-downregulated cells (Fig. 2A). Even when the cells were cultured in medium without osteogenic supplements, the ALP activity and matrix mineralization were enhanced in the H19 group (Fig. 2A). Immunofluorescence staining and Western blot analysis indicated that the protein levels of OCN and Runx2 were upregulated in Lenti-H19-infected hMSCs (Fig. 2B, 2C). As shown by qRT-PCR, the mRNA levels of ALP, OCN, and Runx2 were increased by H19 overexpression, whereas the opposite effects were observed in H19-knockdown hMSCs (Fig. 2D).

miR-675 Promotes OB Differentiation of hMSCs

To determine whether H19-derived miR-675 promoted OB differentiation of hMSCs, lentivirus vectors were used to overexpress exogenous miR-675 or reduce endogenous miR-675. Stably expressing cells were sorted by FACS into miR-NC, miR-675, anti-NC, and anti-miR-675 groups. miR-675-5p and miR-675-3p were increased by approximately 8- and 10-fold, respectively, in the miR-675 group. Suppression of miR-675 by transfection with anti-miR-675 decreased the miR-675-5p and miR-675-3p expression by approximately 50% (Supporting Information Fig. S1C). ALP expression and calcium deposition were increased in miR-675-overexpressed hMSCs. Following OB induction, a similar and stronger tendency was observed. ALP activity and staining were enhanced in the miR-675 group as well as Alizarin red and von Kossa staining. The opposite effects were observed in the miR-675 deficient hMSCs (Fig. 3A). Overexpression of miR-675 increased the mRNA levels of ALP, OCN, and Runx2, and the protein level of Runx2, whereas downregulated miR-675 expression decreased OB marker gene expression (Fig. 3B, 3C).

miR-675 Partially Mediates the Pro-Osteogenic Function of H19

To determine whether the pro-osteogenic effect of H19 was mediated by miR-675, we transfected Lenti-miR-675 into the stably expressing shH19 hMSCs and changed to differentiation medium. Exogenous miR-675 partially rescued the inhibition of ALP activity as well as matrix mineralization in H19-knockdown hMSCs (Fig. 4A). However, the promotion of ALP staining, ALP activity, and matrix mineralization by H19 was lost through mutation of the miR-675 sequence in H19 (Fig. 4B).

H19/miR-675 Downregulates the Expression of TGF-β1

TGF-β1 is a key regulator of cellular differentiation. According to the target-prediction algorithm (RNA22 software), the TGF-β1 transcript contains several putative miR-675-5p and miR-675-3p binding sites (Supporting Information Fig. S2). Among these, miR-675-5p possessed the maximum likelihood for binding to the 5′UTR (588–609 bp) ($\Delta G = -21.9$ kcal/mol), whereas miR-675-3p possessed the maximum likelihood for binding to the CDs (1,126–1,147 bp) ($\Delta G = -21.4$ kcal/mol) (Fig. 5A). Thus, we chose these target sites and separately fused them into a luciferase reporter gene. The 5′UTR reporter activity was reduced by ~50% in the presence of miR-675-5p, and the CDs reporter activity was reduced by ~40% in the presence of miR-675-3p. Mutation of the target sites relieved the repression of reporter activity (Fig. 5B).

Consistently, we transiently transfected miR-675-5p and miR-675-3p mimics into hMSCs and found that the mRNA level of TGF-β1 was reduced by at least 40% in the presence of either miR-675-5p or miR-675-3p (Fig. 5C). The protein expression of TGF-β1 was also decreased in H19/miR-675 overexpressing hMSCs and increased in hMSCs with H19/miR-675 downregulation (Fig. 5D).

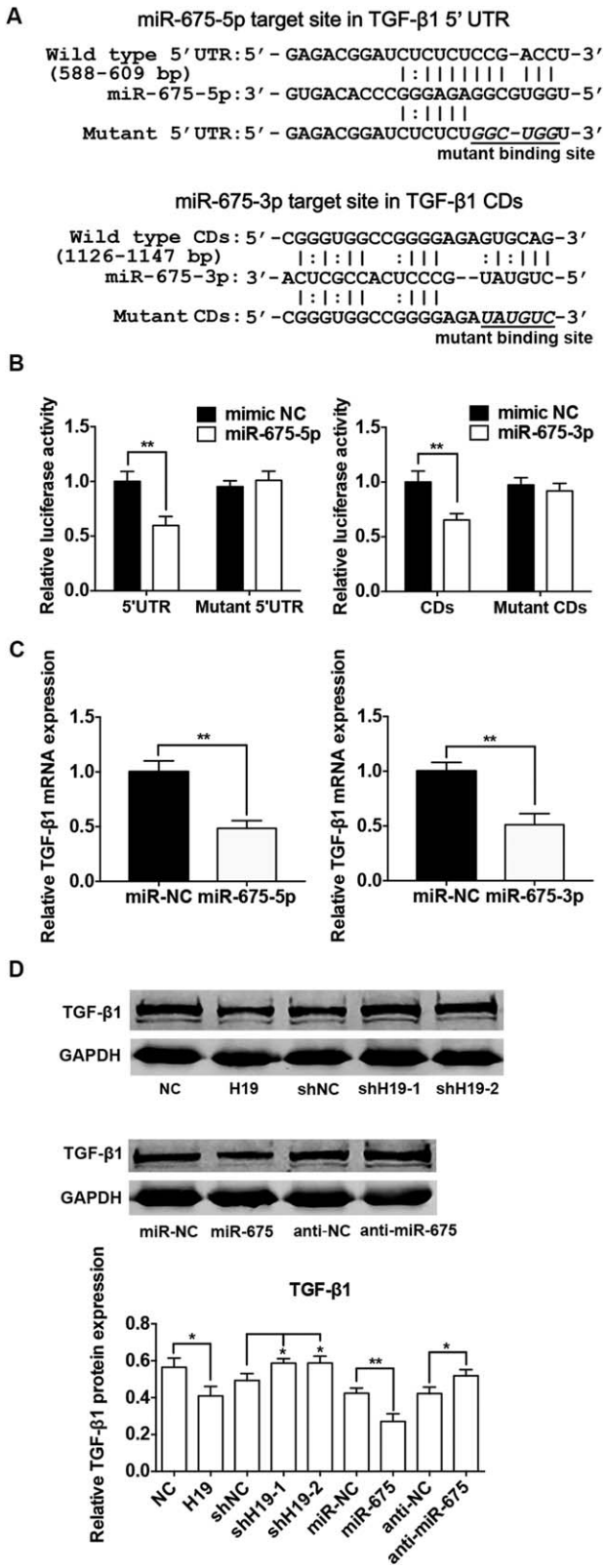

TGF-β1 Inhibits OB Differentiation of hMSCs and Its Effect Depends on HDAC Activity

To evaluate the effects of TGF-β1 on osteogenesis, we first examined its expression pattern. TGF-β1 mRNA level was decreased on the 3rd day and remained at a low level during osteogenic differentiation (Supporting Information Fig. S3A). The protein levels of TGF-β1 and p-Smad3 showed similar changes, with a lag period of 2–3 days (Supporting Information Fig. S3B). Furthermore, we treated hMSCs with exogenous TGF-β1 (2 ng/ml) under osteogenic conditions. TGF-β1 treatment inhibited OB differentiation of hMSCs as assessed by ALP activity, ALP staining, and Alizarin red staining (Supporting Information Fig. S3C). TGF-β1 treatment resulted in transcriptional repression of the ALP and OCN in both GM and OM (Supporting Information Fig. S3D). Previous studies have shown that the inhibition of osteogenesis by TGF-β requires the activity of HDAC4/5 [33]. We then applied TSA (400 nM), an inhibitor of HDAC, together with TGF-β1 to treat hMSCs. TSA overcame the inhibition of OB differentiation by TGF-β1 (Supporting Information Fig. S3C) and rescued the inhibition of ALP and OCN mRNA levels induced by TGF-β1 (Supporting Information Fig. S3D).

H19/miR-675 Downregulates Smad3 Phosphorylation and HDAC4/5 Expression in hMSCs

The Smads act as effectors of TGF-β. HDAC4/5 are directly recruited by Smad3 to the Runx2-binding DNA sequence [33]. To determine whether the downregulation of TGF-β1 induced by H19/miR-675 affects downstream pathways, we assessed the expression of Smad3 by Western blot analysis and showed that Smad3 phosphorylation was reduced in cells overexpressing H19/miR-675 and enhanced in cells with H19/miR-675 downregulation without changing the total level of Smad3 (Fig. 6A). Exogenously applied TGF-β1 (2 ng/ml, 30 minutes) significantly activated the expression of Smad3 phosphorylation in hMSCs (Fig. 6B). Furthermore, qRT-PCR analysis revealed that H19/miR-675 overexpression decreased the mRNA levels of HDAC4/5 (Fig. 6C). Western blot analysis showed that the protein levels of HDAC4/5 were downregulated by H19/miR-675 overexpression and upregulated by H19/miR-675 knockdown in hMSCs (Fig. 6D).

Figure 5. H19/miR-675 downregulated the expression of TGF-β1. **(A):** The seed sequences of miR-675-5p match the 5′UTR of TGF-β1 (upper) and the seed sequences of miR-675-3p match the CD of TGF-β1 (lower). **(B):** The 293T cells were cotransfected with 100 nM miR-675-5p or miR-675-3p or miRNA control (mimic NC) and the luciferase constructs carrying TGF-β1 5′UTR or CDs. Luciferase assays were performed 24 hours after transfection. **(C):** Quantification of mRNA expression of TGF-β1 measured by qRT-PCR in miR-675-5p mimic or miR-675-3p mimic transfected human mesenchymal stem cells relative to the control groups. GAPDH mRNA levels were used for normalization. **(D):** Western blot analysis of protein expression of TGF-β1 and the internal control GAPDH in H19/miR-675 upregulated and downregulated groups. Histograms show the quantification of band intensities. Results are shown as the mean $\pm$ SD (*, $p < .05$; **, $p < .01$). Abbreviations: CD, coding region; GAPDH, glyceraldehyde 3-phosphate dehydrogenase; NC, negative control; TGF-β1, transforming growth factor-β1.

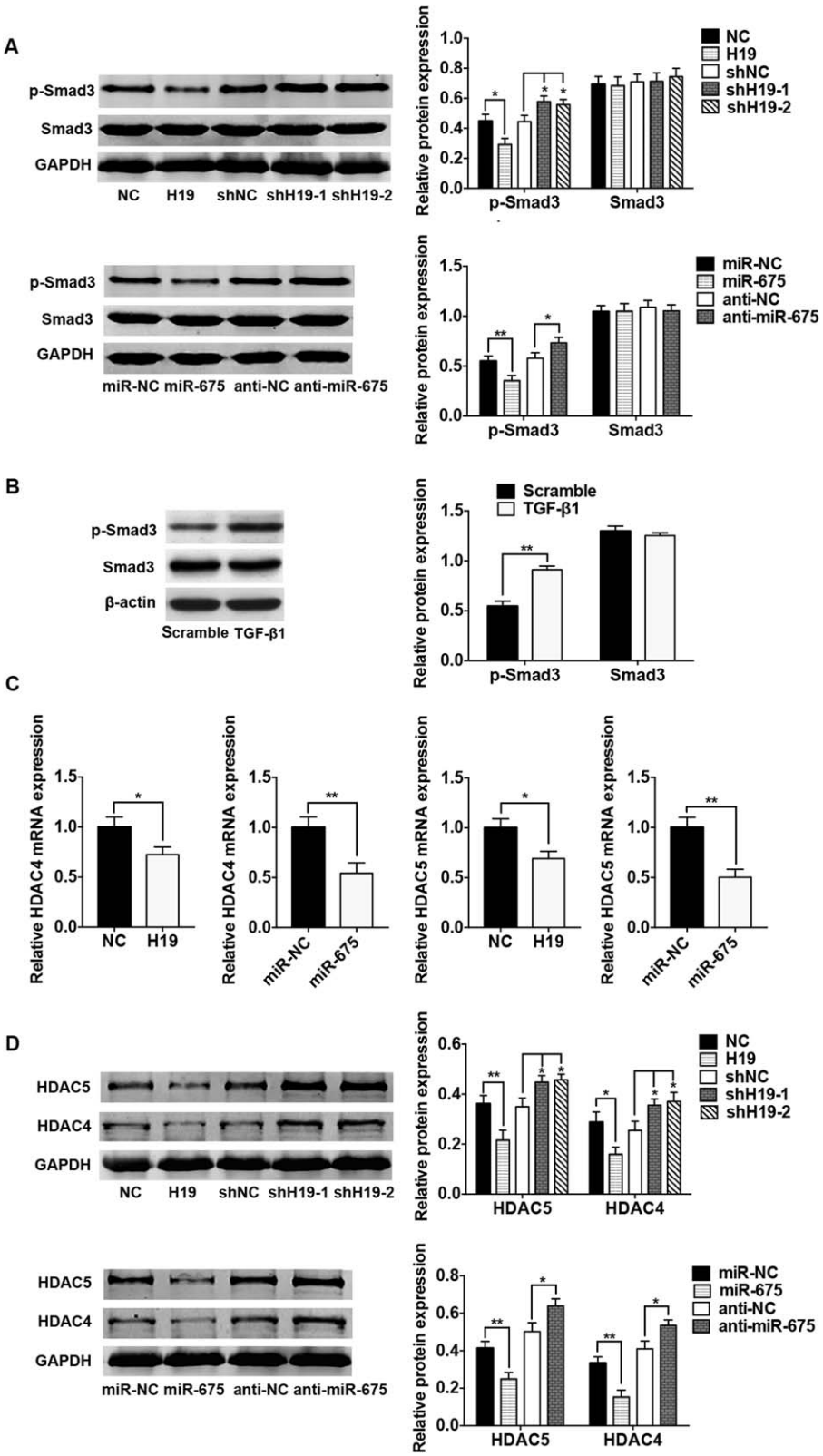

Figure 6. H19/miR-675 downregulated Smad3 phosphorylation and HDAC4/5 expression in human mesenchymal stem cells (hMSCs). **(A):** Western blot analysis (left) and quantification (right) of protein expression of phosphorylated Smad3 (p-Smad3), total Smad3, and GAPDH in H19/miR-675 upregulated or downregulated hMSCs. **(B):** Western blot analysis (left) and quantification (right) of p-Smad3, Smad3, and β-actin expression from hMSCs incubated with or without TGF-β (2 ng/ml) for 30 minutes. **(C):** mRNA levels of HDAC4/5 in the H19 and miR-675 overexpression groups (by qRT-PCR; normalized by GAPDH). **(D):** Western blot analysis (left) and quantification (right) of the protein expression of HDAC4/5, and GAPDH in H19/miR-675 upregulated and downregulated hMSCs. Data are shown as the mean $\pm$ SD (*, $p < .05$; **, $p < .01$). Abbreviations: GAPDH, glyceraldehyde 3-phosphate dehydrogenase; HDAC, histone deacetylase; NC, negative control; TGF-β1, transforming growth factor-β1.

H19 Promotes Bone Formation In Vivo

hMSCs stably expressing H19, shH19-1, and control hMSCs were loaded on Bio-Oss Collagen scaffolds, implanted in the subcutaneous tissue of nude mice (five mice per group), and allowed to grow for 8 weeks (Fig. 7A). Micro-CT showed the BV/TV and BMD were significantly increased in the H19-overexpressing group and decreased in the H19-knockdown group (Fig. 7B). Histological examination corroborated the findings from micro-CT analysis. H&E staining showed that normal lamellar bone with osteocyte lacunae or organized extracellular matrix was formed. The amount of bone tissue was significantly higher in implants containing H19-overexpressing cells than in negative controls, whereas knockdown of H19 decreased bone formation compared with controls (Fig. 7C). Meanwhile, the OBs and bone trabeculae were positive for OCN, as observed in immunohistochemical staining. The size and intensity of staining were increased in the H19-overexpressing group and decreased in the H19-knockdown group (Fig. 7C).

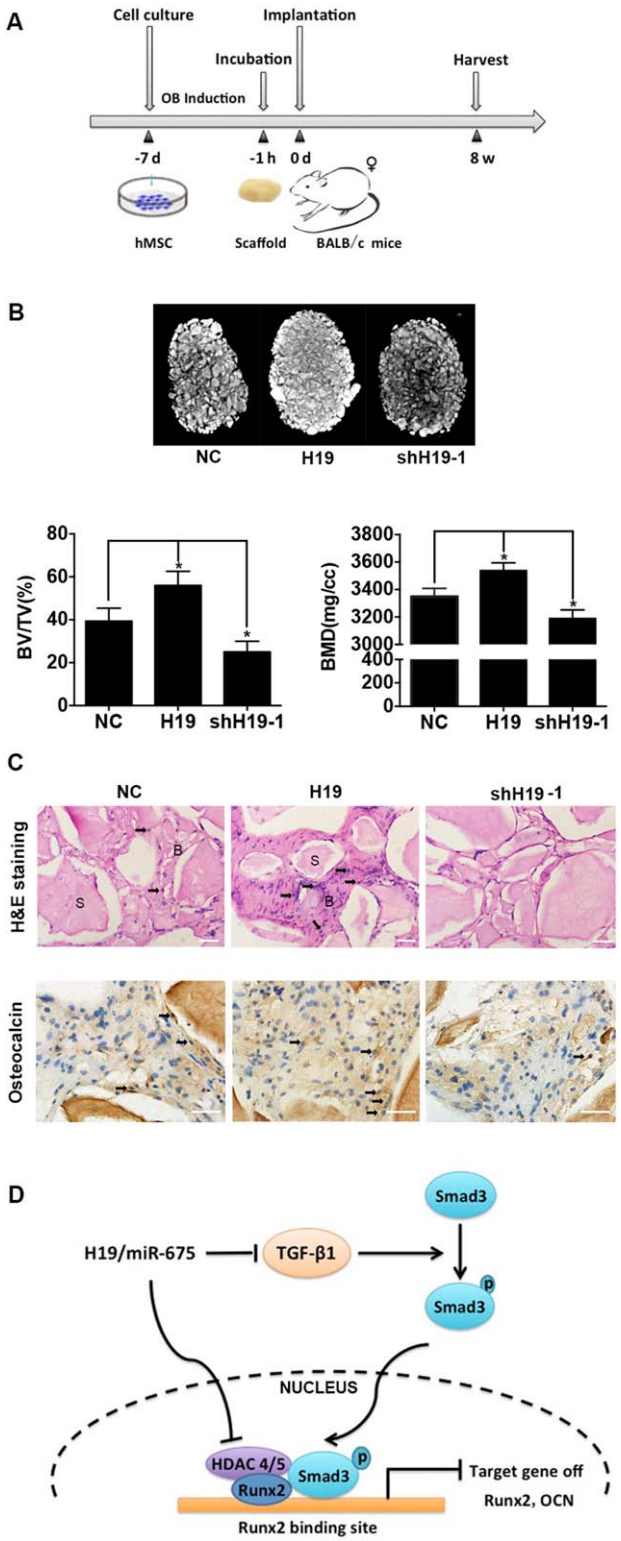

Discussion

This study demonstrated that H19 promotes the osteogenic differentiation of hMSCs. The pro-osteogenic effect of H19 is consistent with the recent study monitoring the lncRNA profile during OB differentiation [12]. Although numerous lncRNAs are known to be involved in carcinogenesis at the transcriptional and post-transcriptional levels [34, 35], only a few have been reported to regulate the osteogenic differentiation of stem cells, such as ANCR [36], HOTTIP [37], and MEG3 [21]. H19 is one of the most abundant and conserved noncoding transcripts in mammalian development [18], and has been demonstrated to promote skeletal muscle differentiation [38]. The importance of H19 in cellular biology and its potential roles in the control of cell or tissue differentiation is under investigation. miR-675 is partially responsible for the pro-osteogenic activity of H19 and enhances bone development in hMSCs. We observed the promotion of OB differentiation as evidenced by ALP activity, ALP staining, and mineralized matrix staining in the presence of miR-675, and miR-675 partially rescued the inhibition of OB differentiation in H19-knockdown cells. These findings indicate that miR-675 partially mediates the pro-osteogenic action of H19. However, the efficiency of miR-675 was less than that of H19. This suggests that other factors or pathways are involved in the regulatory effects of H19 on OB differentiation. Unlike miRNAs, lncRNAs can fold into complex secondary and higher order structures to provide greater potential for target recognition [10, 11, 34]. A single lncRNA may have several modular components. Recently, H19 has been reported to act as a

Figure 7. H19 promoted heterotopic bone formation in vivo. **(A):** Scheme for the heterotopic bone formation procedure. **(B):** Upper: reconstructed three-dimensional micro-CT images of the tissue-engineered bone constructs from NC, H19, and shH19-1 groups. Lower: percentages of new BV/TV and BMD of cultured bone constructs. Data are shown as the mean ± SD (*, $p < .05$). **(C):** H&E staining and immunohistochemical staining of osteocalcin in H19, shH19-1, and NC groups. Note bone formation (B) around the scaffold (S). Osteoblasts are marked with black arrows. Scale bar = 50 μm. **(D):** Schematic of pathways involved in promoting hMSC osteogenic differentiation by H19/miR-675. H19/miR-675 downregulates TGF-β1 expression and subsequently inhibits the phosphorylation of Smad3. H19/miR-675 also downregulates the expression of HDAC4/5 and consequently inhibits the recruitment of HDAC to the Runx2-binding DNA sequence, leading to a reduction in inhibition of the Runx2 target gene. Abbreviations: BMD, bone mineral density; BV/TV, bone volume to tissue volume; hMSC, human mesenchymal stem cell; NC, negative control.

molecular sponge for the let-7 family [39], which is known to regulate bone formation [11]. In addition, H19 is known to be physically associated with EZH2 [40], which is a key regulator of hMSC differentiation processes, including osteogenesis and adipogenesis [41, 42]. Thus, besides generating miR-675, H19 may interact with different molecules involved in the complex biology of OB differentiation and bone formation that require the coordination of a large number of genes controlling cell proliferation, cell differentiation, bone matrix production, and matrix mineralization.

H19/miR-675 promotes osteogenic differentiation by negatively regulating TGF-β1. Interestingly, a recent study showed that miR-675 directly targets the 3′UTR of transforming growth factor β-induced protein (TGFBI) in prostate cancer metastasis [43]. It seems that H19/miR-675 regulates several targets in the TGF-β signaling pathway. TGF-β is known for its critical roles in cellular differentiation [44]. Although the regulation of TGF-β in bone development and remodeling has been addressed, the effect on OB differentiation remains unclear. TGF-β seems to stimulate proliferation and early differentiation of OB, but inhibits its terminal differentiation [45, 46]. The precise response may depend on the extracellular milieu, cell density, and the differentiation stage of the cells [47]. In this study, we found that TGF-β1 remained at a low level after OB induction, and exogenous TGF-β1 treatment inhibited osteogenic differentiation, consistent with previous studies showing that TGF-β inhibits the expression of ALP and OCN [33, 46, 48]. H19 and miR-675 promoted osteogenesis at least partially through the downregulation of TGF-β1.

H19/miR-675 downregulates Smad3 phosphorylation and HDAC4/5 expression. TGF-β phosphorylates Smad3 [49], which then recruits HDAC4/5 to Runx2 and forms a stable complex at the Runx2-binding DNA sequence, thereby downregulating Runx2 and OCN gene expression [33]. H19/miR-675 not only downregulated Smad3 phosphorylation to reduce the recruitment of HDAC to the Runx2 target gene, but also inhibited HDAC4/5 expression. This effect significantly inhibited the activity of HDAC and thus inhibited the deacetylation of histone H4 at the endogenous OCN promoter induced by TGF-β1 [33]. TSA inhibited the activity of HDAC and thus blocked the inhibition of osteogenic differentiation induced by TGF-β1, similar to the effect of H19/miR-675 in hMSCs. However, whether miR-675 inhibits the expression of HDAC4/5 by directly targeting these genes or through another mechanism requires further investigation.

There is increasing interest in developing a novel approach for therapeutics based on lncRNAs by modifying their expression. One preclinical study of H19 knockdown in embryonic stem cells demonstrates the possibility of cell-based therapy for muscular atrophy [50]. Our study provides important insights into the trans-regulatory function of H19 in OB differentiation both in vitro and in a model of heterotopic bone formation. miR-675 is partially responsible for this pro-osteogenic effect of H19 via the TGF-β1/Smad3/HDAC pathway. Thus, it is possible to upregulate the expression of H19/miR-675 in hMSCs to enhance local bone formation.

Summary

Our results demonstrated that lncRNA H19 promoted OB differentiation and bone formation of hMSCs, and miR-675 partially mediated H19-induced pro-osteogenic activity. H19/miR-675 not only downregulated TGF-β1 and subsequently inhibited Smad3 phosphorylation, but also downregulated HDAC4/5 expression to enhance the expression of osteogenic markers. Based on these results, altering the H19/miR-675 level may provide a novel approach to enhance local bone formation.

Acknowledgments

This work was supported by the National Natural Science Foundation of China (81402235) and Foundation of Peking University School and Hospital of Stomatology (PKUSS20140104).

Author Contributions

Y.H.: conception and design, collection and/or assembly of data, data analysis and interpretation, and manuscript writing; Y.Z.: conception and design and collection and/or assembly of data; L.J.: conception and design, data analysis and interpretation, financial support, and manuscript writing; W.L.: financial support and final approval of manuscript. Y.H. and Y.Z. contributed equally to this work.

Disclosure of Potential Conflicts of Interest

The authors indicate no potential conflicts of interest.

References

1 Pittenger MF, Mackay AM, Beck SC et al. Multilineage potential of adult human mesenchymal stem cells. Science 1999;284:143–147.

2 Phinney DG, Prockop DJ. Concise review: Mesenchymal stem/multipotent stromal cells: The state of transdifferentiation and modes of tissue repair—Current views. Stem Cells 2007;25:2896–2902.

3 Rastegar F, Shenaq D, Huang J et al. Mesenchymal stem cells: Molecular characteristics and clinical applications. World J Stem Cells 2010;2:67–80.

4 Macchiarini P, Jungebluth P, Go T et al. Clinical transplantation of a tissue-engineered airway. Lancet 2008;372:2023–2030.

5 Mattick JS. RNA regulation: A new genetics? Nat Rev Genet 2004;5:316–323.

6 Li Z, Hassan MQ, Jafferji M et al. Biological functions of miR-29b contribute to positive regulation of osteoblast differentiation. J Biol Chem 2009;284:15676–15684.

7 Chen L, Holmstrom K, Qiu W et al. MicroRNA-34a inhibits osteoblast differentiation and in vivo bone formation of human stromal stem cells. Stem Cells 2014;32:902–912.

8 Hwang S, Park SK, Lee HY et al. miR-140-5p suppresses BMP2-mediated osteogenesis in undifferentiated human mesenchymal stem cells. FEBS Lett 2014;588:2957–2963.

9 Kureel J, Dixit M, Tyagi AM et al. miR-542-3p suppresses osteoblast cell proliferation and differentiation, targets BMP-7 signaling and inhibits bone formation. Cell Death Dis 2014;5:e1050.

10 Hung T, Chang HY. Long noncoding RNA in genome regulation: Prospects and mechanisms. RNA Biol 2010;7:582–585.

11 Li X, Wu Z, Fu X et al. lncRNAs: Insights into their function and mechanics in underlying disorders. Mutat Res Rev Mutat Res 2014;762:1–21.

12 Wang L, Wang Y, Li Z et al. Differential expression of long noncoding ribonucleic acids during osteogenic differentiation of human bone marrow mesenchymal stem cells. Int Orthop 2015;39:1013–1019.

13 Zhang Y, Tycko B. Monoallelic expression of the human H19 gene. Nat Genet 1992;1:40–44.

14 Hurst LD, Smith NG. Molecular evolutionary evidence that H19 mRNA is functional. Trends Genet 1999;15:134–135.
15 Wilusz JE, Sunwoo H, Spector DL. Long noncoding RNAs: Functional surprises from the RNA world. Genes Dev 2009;23:1494–1504.
16 Bartel DP. MicroRNAs: Target recognition and regulatory functions. Cell 2009;136:215–233.
17 Huntzinger E, Izaurralde E. Gene silencing by microRNAs: Contributions of translational repression and mRNA decay. Nat Rev Genet 2011;12:99–110.
18 Gabory A, Jammes H, Dandolo L. The H19 locus: Role of an imprinted non-coding RNA in growth and development. BioEssays 2010;32:473–480.
19 Cai X, Cullen BR. The imprinted H19 noncoding RNA is a primary microRNA precursor. RNA 2007;13:313–316.
20 Dudek KA, Lafont JE, Martinez-Sanchez A et al. Type II collagen expression is regulated by tissue-specific miR-675 in human articular chondrocytes. J Biol Chem 2010; 285:24381–24387.
21 Zhuang W, Ge X, Yang S et al. Upregulation of lncRNA MEG3 promotes osteogenic differentiation of mesenchymal stem cells from multiple myeloma patients by targeting BMP4 transcription. Stem Cells 2015;33:1985–1997.
22 Jia LF, Wei SB, Mitchelson K et al. miR-34a inhibits migration and invasion of tongue squamous cell carcinoma via targeting MMP9 and MMP14. PLoS One 2014;9:e108435.
23 Ge W, Shi L, Zhou Y et al. Inhibition of osteogenic differentiation of human adipose-derived stromal cells by retinoblastoma binding protein 2 repression of RUNX2-activated transcription. Stem Cells 2011;29: 1112–1125.
24 Ge W, Liu Y, Chen T et al. The epigenetic promotion of osteogenic differentiation of human adipose-derived stem cells by the genetic and chemical blockade of histone demethylase LSD1. Biomaterials 2014;35: 6015–6025.
25 Bhargava U, Bar-Lev M, Bellows CG et al. Ultrastructural analysis of bone nodules formed in vitro by isolated fetal rat calvaria cells. Bone 1988;9:155–163.
26 Wei J, Li H, Wang S et al. let-7 enhances osteogenesis and bone formation while repressing adipogenesis of human stromal/mesenchymal stem cells by regulating HMGA2. Stem Cells Dev 2014;23:1452–1463.
27 Jia LF, Wei SB, Gan YH et al. Expression, regulation and roles of miR-26a and MEG3 in tongue squamous cell carcinoma. Int J Cancer 2014;135:2282–2293.
28 Zhou H, Rigoutsos I. MiR-103a-3p targets the 5′ UTR of GPRC5A in pancreatic cells. RNA 2014;20:1431–1439.
29 Yu BH, Zhou Q, Wang ZL. Periodontal ligament versus bone marrow mesenchymal stem cells in combination with Bio-Oss scaffolds for ectopic and in situ bone formation: A comparative study in the rat. J Biomater Appl 2014;29:243–253.
30 Lai RF, Li ZJ, Zhou ZY et al. Effect of rhBMP-2 sustained-release nanocapsules on the ectopic osteogenesis process in Sprague-Dawley rats. Asian Pac J Trop Med 2013;6: 884–888.
31 Ma SY, Feng ZQ, Lai RF et al. Synergistic effect of RhBMP-2 and bFGF on ectopic osteogenesis in mice. Asian Pac J Trop Med 2015;8:53–59.
32 Kempen DH, Lu L, Hefferan TE et al. Enhanced bone morphogenetic protein-2-induced ectopic and orthotopic bone formation by intermittent parathyroid hormone (1-34) administration. Tissue Eng Part A 2010; 16:3769–3777.
33 Kang JS, Alliston T, Delston R et al. Repression of Runx2 function by TGF-beta through recruitment of class II histone deacetylases by Smad3. EMBO J 2005;24:2543–2555.
34 Wapinski O, Chang HY. Long noncoding RNAs and human disease. Trends Cell Biol 2011;21:354–361.
35 Esteller M. Non-coding RNAs in human disease. Nat Rev Genet 2011;12:861–874.
36 Zhu L, Xu PC. Downregulated LncRNA-ANCR promotes osteoblast differentiation by targeting EZH2 and regulating Runx2 expression. Biochem Biophys Res Commun 2013; 432:612–617.
37 Wang KC, Yang YW, Liu B et al. A long noncoding RNA maintains active chromatin to coordinate homeotic gene expression. Nature 2011;472:120–124.
38 Dey BK, Pfeifer K, Dutta A. The H19 long noncoding RNA gives rise to microRNAs miR-675-3p and miR-675-5p to promote skeletal muscle differentiation and regeneration. Genes Dev 2014;28:491–501.
39 Kallen AN, Zhou XB, Xu J et al. The imprinted H19 lncRNA antagonizes let-7 microRNAs. Mol Cell 2013;52:101–112.
40 Luo M, Li Z, Wang W et al. Long non-coding RNA H19 increases bladder cancer metastasis by associating with EZH2 and inhibiting E-cadherin expression. Cancer Lett 2013;333:213–221.
41 Hemming S, Cakouros D, Isenmann S et al. EZH2 and KDM6A act as an epigenetic switch to regulate mesenchymal stem cell lineage specification. Stem Cells 2014;32:802–815.
42 Chen YH, Yeh FL, Yeh SP et al. Myocyte enhancer factor-2 interacting transcriptional repressor (MITR) is a switch that promotes osteogenesis and inhibits adipogenesis of mesenchymal stem cells by inactivating peroxisome proliferator-activated receptor gamma-2. J Biol Chem 2011;286:10671–10680.
43 Zhu M, Chen Q, Liu X et al. lncRNA H19/miR-675 axis represses prostate cancer metastasis by targeting TGFBI. FEBS J 2014; 281:3766–3775.
44 James D, Levine AJ, Besser D et al. TGFbeta/activin/nodal signaling is necessary for the maintenance of pluripotency in human embryonic stem cells. Development 2005;132:1273–1282.
45 Bonewald LF, Dallas SL. Role of active and latent transforming growth factor beta in bone formation. J Cell Biochem 1994;55: 350–357.
46 Centrella M, Horowitz MC, Wozney JM et al. Transforming growth factor-beta gene family members and bone. Endocr Rev 1994; 15:27–39.
47 Suzuki E, Ochiai-Shino H, Aoki H et al. Akt activation is required for TGF-beta1-induced osteoblast differentiation of MC3T3-E1 pre-osteoblasts. PLoS One 2014;9: e112566.
48 Alliston T, Choy L, Ducy P et al. TGF-beta-induced repression of CBFA1 by Smad3 decreases cbfa1 and osteocalcin expression and inhibits osteoblast differentiation. EMBO J 2001;20:2254–2272.
49 Derynck R, Zhang YE. Smad-dependent and Smad-independent pathways in TGF-beta family signalling. Nature 2003;425:577–584.
50 Kwak M, Hong S, Yu SL et al. Parthenogenetic embryonic stem cells with H19 siRNA-mediated knockdown as a potential resource for cell therapy. Int J Mol Med 2012;29:257–262.


See www.StemCells.com for supporting information available online.